Dalton Transactions

PERSPECTIVE

View Article Online
View Journal

Cite this: DOI: 10.1039/c8dt01966e

Gold nanocatalysts supported on carbon for electrocatalytic oxidation of organic molecules including guanines in DNA

Zheng Chang, †[a,c] Yue Yang,†[b,c] Jie He *[c,d] and James F. Rusling *[c,d,e,f]

Received 16th May 2018,
Accepted 20th July 2018

DOI: 10.1039/c8dt01966e

rsc.li/dalton

Gold (Au) is chemically stable and resistant to oxidation. Although bulk Au is catalytically inert, nanostructured Au exhibits unique size-dependent catalytic activity. When Au nanocatalysts are supported on conductive carbon (denoted as Au@C), Au@C becomes promising for a wide range of electrochemical reactions such as electrooxidation of alcohols and electroreduction of carbon dioxide. In this mini-review, we summarize Au@C nanocatalysts with specific attention on the most recent achievements including the findings in our own laboratories, and show that Au nanoclusters (AuNCs, <2 nm) on nitrided carbon are excellent electrocatalysts for the oxidation of organic molecules including guanines in DNA. The state-of-the-art synthesis and characterization of these nanomaterials are also documented. Synergistic interactions among Au-containing multicomponents on carbon supports and their applications in electrocatalysis are discussed as well. Finally, challenges and future outlook for these emerging and promising nanomaterials are envisaged.

[a]Department of Applied Chemistry of College of Science, Xi'an University of Technology, Xi'an 710054, China
[b]Department of Chemical Engineering, Nanjing University of Science and Technology, Jiangsu 210094, China
[c]Department of Chemistry, University of Connecticut, Storrs, CT 06269, USA. E-mail: jie.he@uconn.edu, james.rusling@uconn.edu
[d]Institute of Materials Science, University of Connecticut, Storrs, CT 06269, USA
[e]Department of Surgery and Neag Cancer Center, UConn Health, Farmington, CT 06032, USA
[f]School of Chemistry, National University of Ireland at Galway, Galway H91 TK33, Ireland
†These authors contributed equally.

1. Introduction

Gold (Au) is chemically stable and resistant to oxidation. When it has a particle size in the low nanometer range, nanostructured Au with unique size-dependent catalytic properties that differ from those of its bulk counterpart has attracted considerable attention in catalysis.[1-4] Relevant to this review, early examples reported by Haruta and others showed that small Au nanoparticles (AuNPs, <5 nm) supported on a number of metal oxides are extremely active for low-temperature CO

Zheng Chang

Zheng Chang is a lecturer at the Department of Applied Chemistry of College of Science, Xi'an University of Technology, China. She is currently working with Professors Jie He and James F. Rusling at the Department of Chemistry, University of Connecticut (USA) as a visiting Professor. She received a PhD in Chemistry at Northwest University (China) in 2011. Her research focuses on the design and synthesis of functional nanoparticles and their applications in bioelectroanalytical chemistry and luminescence analysis.

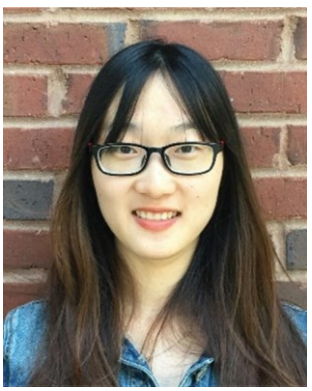

Yue Yang

Yue Yang is a PhD student of Materials Science and Engineering at Nanjing University of Science and Technology (NUST), China. She currently works in the Hybrid Materials Laboratory with Dr Jie He at the University of Connecticut as a visiting student. She obtained her BSc degree in chemistry from NUST in 2015. Her current research interests focus on the synthesis of bimetallic and transition metal oxide nanomaterials to understand their electrochemistry for applications in fuel cells and clean energy.

oxidation,[5-7] CO_2 hydrogenation,[8] catalytic combustion of methanol,[9] NO reduction,[10] selective epoxidation of propene,[11] low-temperature water gas shift reactions,[12] etc. All these results point out that AuNPs with a small size (<5 nm) are usually more catalytically active compared to larger ones (>10 nm).[13] Atomically precise alkylthiol-protected Au nanoclusters (AuNCs, e.g., Au_{25}, Au_{38} and Au_{144}) with excellent size control have been synthesized later via wet-chemical reduction. This further allows quantifying size-dependent catalytic performance.[14,15]

In addition to the intrinsic size effect, the activity of Au nanocatalysts can be influenced by the nature and morphology of supports.[16,17] The primary role of the support is to anchor nanoparticles (NPs) onto its surface, preventing the NPs from sintering and agglomerating during catalytic reactions. Supported Au nanocatalysts can be very stable and resistant from corrosion in harsh environments like strong acid/base and high temperature. There are many different types of supports used for adsorption and stabilization of AuNPs, such as metal oxide powder,[18-21] magnetic microspheres,[22,23] polymer nanospheres or nanofibers,[24-26] mesoporous silica,[27,28] carbonaceous supports,[29-33] etc. Low-cost carbon supports have shown to be superior compared to other supports in terms of their conductivity, the cost of raw materials, resistance to strong acid or base and the possibility to control porosity and surface chemistry.[34,35] A good example of the influence of the support was shown by Benkó et al., where carbon-supported Au nanocatalysts (denoted Au@C) outperformed other Au nanocatalysts supported on TiO_2, SiO_2 and CeO_2 in CO oxidation and glucose oxidation reactions.[35]

Various kinds of carbon materials have been extensively studied in electrocatalysis,[36,37] including carbon nanotubes (CNTs),[38] carbon nanofibers,[39] two-dimensional graphene oxide/reduced graphene oxide (GO/RGO),[40] mesoporous carbon and hollow carbon nanospheres (HCNS),[41,42] metal-organic framework (MOF)-derived carbonaceous materials,[43] etc. The merits of simple synthesis and superior conductivity have enormously enriched the practical applications of carbon supported noble metal nanocatalysts in electrocatalysis.[44-46] On the other hand, due to the relatively inert nature of carbon and the weak interaction between Au and the support, AuNPs tend to overgrow and aggregate. Thus, the modification and functionalization of the carbon surface, such as the introduction of hydroxyl groups and heteroatom doping, have become useful tools to enhance the interaction of Au and carbon and thus to stabilize AuNPs supported on carbon. In addition, the synergistic effect of Au/support may vary the charge state of AuNPs, resulting in an electron-rich NP surface. In a recent study, we showed that electron-rich AuNCs supported on nitrided carbon supports favor the adsorption of electrophile reactants like CO_2; therefore, this can promote the activity and selectivity for CO_2 electroreduction in comparison with AuNCs on pristine carbon, due to the strong electronic interaction of Au/support.[47] This will be discussed in detail in Section 2.3.

Au-Based multicomponent nanocatalysts have attracted much attention and benefited from the controllable synthesis of bimetallic or multimetallic NPs. So, a second metal, such as Ag, Co, Cu, Ni, Pd, Pt, Sn, etc., has been introduced in the syntheses to form Au-based binary or multicomponent nanocatalysts. It has been an efficient strategy to reduce the noble metal loading and show a remarkable enhancement of electrocatalytic activity due to the multifunctionality synergistic effects.[48,49] As briefly summarized in Table 1, a variety of heterogeneous reactions can be catalyzed by using multicomponent nanocatalysts.[30,32,50-65] For example, incorporation of Pt and Pd with Au can usually promote electrochemical reactions like methanol oxidation and oxygen reduction. Meanwhile, the presence of Au could retain effective CO tolerance during the catalytic reaction.[57,64]

The remainder of this review will discuss typical synthetic routes for Au@C nanocatalysts. Next, we will focus on their fascinating applications for various electrocatalytic oxidative


Jie He

Jie He received his BS and MS degrees in Polymer Materials from Sichuan University and his PhD in Chemistry from Universite de Sherbrooke with Professor Yue Zhao. He then worked as a postdoctoral fellow at the University of Maryland with Professor Zhihong Nie. In 2014, he joined the faculty of the University of Connecticut where he is currently an Assistant Professor in Chemistry Department. His research focuses on the design and synthesis of polymer/inorganic hybrid materials for bioinspired catalysis and renewable energy conversion.

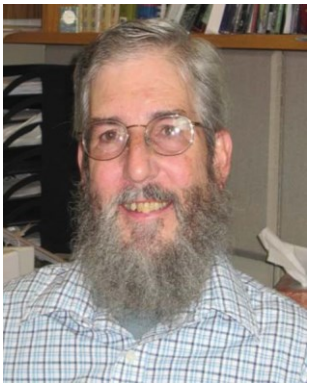
James F. Rusling

James f. Rusling obtained his B.Sc. degree in Chemistry from Drexel University in 1969, and Ph. D. from Clarkson University in 1979. He is a Professor of Chemistry at the University of Connecticut and a Professor of Surgery at UConn Health. His current research includes the development of nano-science based arrays for cancer diagnostics, electro-optical and LC-MS/MS arrays for toxicity screening, and fundamental bioelectrochemistry. He has authored over 400 research papers and several books, and he is an accomplished musician interested in Irish and American folk styles.

Table 1 Summary of catalytic reactions using carbon-supported Au-based multicomponent nanocatalysts

Catalyst composition	Carbonaceous type	Catalytic reaction	Ref.
AuCs	Activated carbon	Acetylene hydrochlorination	50
Pd_xAu_{1-x}	Vulcan XC-72	Borohydride oxidation	30
AuPd	Vulcan XC-72	CO and H_2 oxidation	51
AuPd	Activated carbon	Toluene oxidation	52
AuPd	RGO	O_2 reduction	53
AuPd	Vulcan XC-72	H_2, CO oxidation	54
$Pd_1Au_{24}(SC_{12}H_{25})_{18}$	CNTs	Benzyl alcohol oxidation	55
$AuPd_4$	Vulcan XC-72	Ethanol oxidation	58
Pd@Au	Vulcan XC-72	Ethanol oxidation	62
AuPt	Graphene	O_2 reduction, methanol oxidation	32
AuPt	Vulcan XC-72	Methanol oxidation	56
AuPt	Vulcan XC-72R	O_2 reduction	57
AuPt	Vulcan XC-72R	CO oxidation	61
AuPt	Carbon black	Methanol oxidation	64
Pd-Co-M (M = Pt, Au, Ag)	Vulcan XC-72R	O_2 reduction	59
Au-Co(III)-Cu(II)	Spherical activated carbon (SAC)	Acetylene hydrochlorination	60
NiPdAu	Vulcan XC-72R	Methanol oxidation	63
$Pt_xM_yAu_z$ (M = Ni, Cu, Co)	Vulcan XC-72	O_2 reduction	65

reactions. At the end of the article, we analyze the current problems and future perspectives in this area. We hope that this review will help readers to gain insight into the design and applications of well-defined Au nanocatalysts for electrocatalysis.

2. Synthesis of AuNPs supported on carbon materials

The intrinsic physicochemical properties of AuNPs are largely influenced by their size and morphology. Considerable efforts have been devoted to the precise control over the size, shape, stability, and functionality of monodisperse AuNPs supported on carbon through the following two methods. First, one can synthesize AuNPs primarily through wet-chemistry reduction of precursors, and then assembling pre-synthesized AuNPs onto the carbon surface. This is also known as the "self-assembly" method. It allows one to predesign the size, shape and chemical composition of AuNPs using the well-developed colloidal synthesis method. However the catalytic performance and stability of these prepared AuNPs often suffer from: (i) surface ligands that block the electron transfer for electrocatalysis; and (ii) the weak interaction with the carbon support that destabilizes AuNPs and thus leads to sintering during the reaction. Later on, the "direct growth" method has been developed as a means to solve these problems. However, the direct growth of AuNPs on carbon does not offer any control over the size of AuNPs. To resolve the large dispersity of AuNPs in the "direct growth" method, doping techniques of carbon with various heteroatoms are developed to enhance the interaction between AuNPs and carbon. For example, the "soft nitriding" method, which effectively modifies the surface of carbon with N, emerged recently as demanded. As such, the nucleation rate of Au is significantly enhanced on nitrided carbon resulting in the formation of ultrasmall AuNCs with a diameter <2 nm. Doping techniques to modify the carbon surface also ensure a strong interaction between Au and carbon to stabilize AuNPs in the course of electrocatalysis. In this section, we will summarize and discuss the synthetic strategies for Au supported on carbon nanomaterials.

2.1. Self-assembly method

The self-assembly of AuNPs on carbon supports involves the synthesis of Au colloids in solution and the subsequent assembly of the as-resulting AuNPs on the functionalized carbon support. This allows one to predesign the nanostructures of AuNPs using various synthetic methods developed to date. The self-assembly of AuNPs on carbon is often triggered by non-covalent interactions, such as electrostatic attraction, hydrophobic interactions, hydrogen-bonding interactions and coordination. For example, CNTs or GO treated with concentrated HNO_3 or a H_2SO_4-HNO_3 mixture can produce carboxylic acid and hydroxyl groups on the surface of carbon.[66] The negatively charged carbon surface is able to physically adsorb AuNPs capped with positively charged ligands through electrostatic attraction. This method has been widely used to assemble AuNPs on GO due to the negatively charged GO surface.[67-70] Through the self-assembly approach, AuNPs with a size of 3.5, 9 and 25 nm prepared via the chemical reduction of $NaBH_4$ can uniformly self-assemble on GO sheets.[69] Surface charge of carbon can be introduced through the layer-by-layer technique. For instance, positively charged AuNPs (a zeta potential of +32.4 mV, pH 7) can self-assemble on functionalized multiwalled carbon nanotubes (MWCNTs) coated with a negatively charged poly(diallyldimethylammonium chloride)/poly(sodium 4-styrenesulfonate) (PDAC/PSS) bilayer (a zeta potential of −46.2 mV, pH 7) via the electrostatic interaction as reported by Kim et al.[71] By tailoring the surface of carbon to be positively charged by adsorbing cationic polyelectrolytes, negatively charged AuNPs can be adsorbed on the CNTs as well.[72-74]

Another example by Han and co-workers shows the pre-synthesized 2 nm AuNPs capped with a decanethiol (DT) monolayer shell assembled on CNTs in the presence of the

mediating linker 11-mercaptoundecanoic acid/1,9-nonanedithiol.[75] A combination of hydrophobic interactions and hydrogen bonding interactions between the alkyl chains/carboxylic groups of capping/linking agents and surface functional groups of CNTs drove the assembly of AuNPs on CNTs.

Huang and co-workers demonstrated the high-density self-assembly of AuNPs on the surface of MWCNTs without any pretreatment of the carbon support.[76] They used 1-pyrenemethylamine as the linker where the alkylamine substituent of the pyrene bound to AuNPs; meanwhile, the pyrene fluorophore bound to MWCNTs via π-π stacking. Shi et al. established a simple method to disperse AuNPs on CNTs in aqueous solution by sonication without any acid oxidation or functionalization of CNTs (Fig. 1). A small amount of ethanol was added into an aqueous suspension of CNTs to reduce the interfacial tension between CNTs and water, thereby changing the wettability of hydrophobic CNTs and enhancing the interaction between CNTs and AuNPs.[77]

In addition to monometallic AuNPs, Au-based bimetallic NPs have been reported by many groups to self-assemble on the surface of carbon. For example, Han et al. reported that Au-Pd alloy NPs capped with poly(vinyl alcohol) (PVA) adsorbed on g-C_3N_4 by a simple mixing process (Fig. 2).[78] Lin's group reported the loading of 3.3 nm Au-Pt alloy NPs on graphene nanosheets and XC-72 carbon black with the assistance of poly(diallyldimethylammonium chloride) (PDDA).[79] The as-synthesized Ag@Au and Fe@Au NPs attached onto p-aminothiophenol (PATP)-functionalized GO sheets to obtain bimetal-graphene nanocomposites were also prepared by Gupta and co-workers.[80,81]

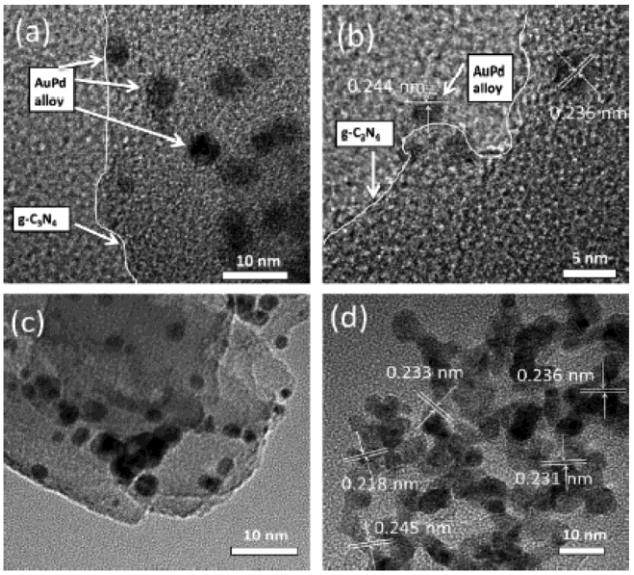

Fig. 2 High-resolution TEM images of the as-prepared AuPd/g-C_3N_4 (a–c) and unsupported AuPd NP samples (d). Reprinted with permission from ref. 78. Copyright 2015, Elsevier.

2.2. Direct growth method

The direct growth of metal NPs or nanoclusters on supports is a classical route to highly dispersed supported nanocatalysts. Taking AuNPs supported on GO as an example, in situ reduction of gold salts on support materials with reducing agents like BH_4^-, sodium citrate and ascorbic acid can result in the growth of AuNPs attached on GO. The growth of AuNPs on graphene has been reported by Goncalves[82] and Pocklanova[83] where sodium citrate was used as a reductant for $AuCl_4^-$ in the presence of RGO. However, the produced AuNPs usually have a broad size distribution and relatively large size (a few to tens of nanometers). Zhang and co-workers developed a one-pot synthesis of 7 nm AuNPs on RGO using sodium citrate as the reductant and stabilizer simultaneously.[84] Sodium citrate can reduce both GO and Au precursors, and prevent the formation of agglomerates/overgrowth of AuNPs. Other than graphene nanosheets, activated carbon is also a choice for the in situ growth of AuNPs. Yan et al. reported that AuNPs in the range of 2 to 16 nm supported on activated carbon were prepared by rapid reduction of $AuCl_4^-$ on the surface of activated carbon with KBH_4 in the presence of polyvinylpyrrolidone (PVP) (Fig. 3).[85]

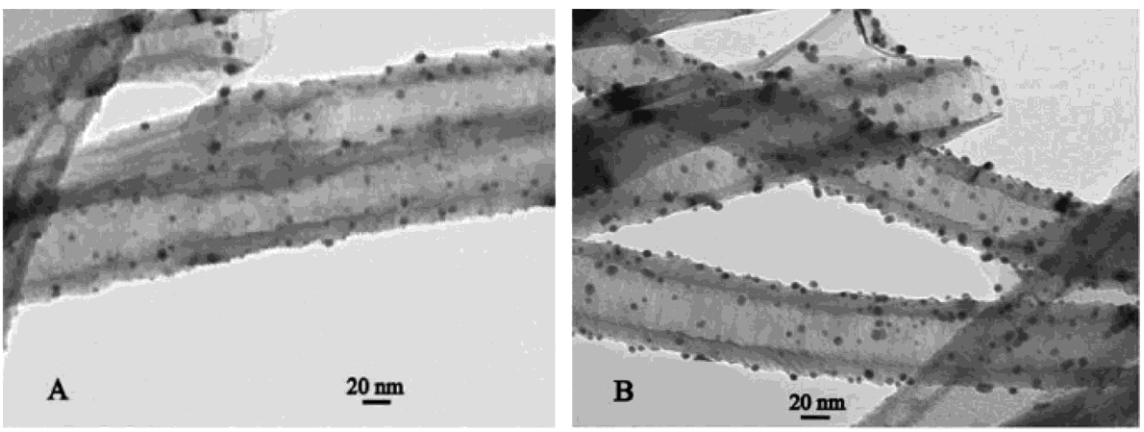

Fig. 1 Transmission electron microscopy (TEM) images of Au@CNTs with a loading ratio of (A) 5 wt% and (B) 10 wt%. Reprinted with permission from ref. 77. Copyright 2009, Elsevier.

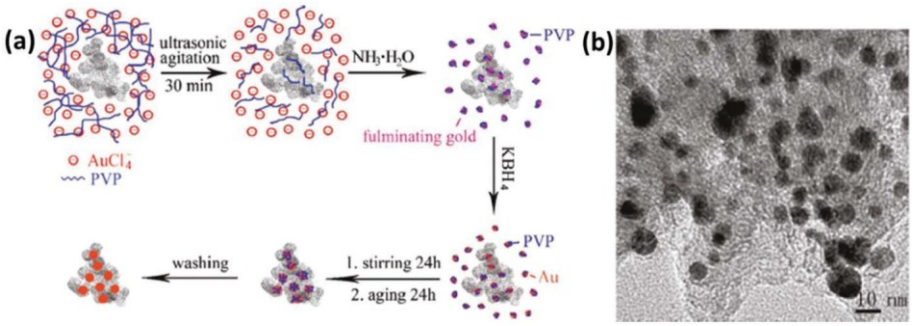

Fig. 3 (a) Schematic illustration of the synthesis of the Au@C nanocatalyst; (b) TEM image of the Au@C nanocatalyst. Reprinted (adapted) with permission from ref. 85. Copyright 2011, American Chemical Society.

These direct growth syntheses suffer from poor control over the Au size and morphology, and particularly limit the applications of Au@C as nanocatalysts, since AuNPs with a size >5 nm are less active. To control the size of Au, various stabilizers and surfactants are required to precisely control the size and shape of AuNPs, enhance the interaction between the NPs and supports, and prevent the overgrowth of AuNPs.[2,86,87] Huang et al. developed an efficient synthetic method for in situ growth of 1-octadecanethiol (ODT) capped AuNCs on GO nanosheets by photoirradiation.[88] AuNCs with a size of 1.2 ± 0.3 nm were distributed in an ordered pattern where the distance between the particle chains was ~4.4 nm. This was attributed to the linear thiol ODT self-assembled along the ⟨100⟩ direction on graphene surfaces.

Surfactants, however, cover the surface of AuNPs that inevitably blocks the surface catalytically active sites and essentially slows or shuts down the electron transfer. This is detrimental for electrocatalytic performance.[89,90] Therefore, surfactant-free synthetic methods are highly desirable to overcome such a challenge. For example, 12.8 ± 2.5 nm AuNPs on GO sheets can be synthesized using hydrothermal reduction of $HAuCl_4$ in an aqueous NaOH/GO mixture at 180 °C for 12 h.[91] Another example by Shao et al. showed well-dispersed AuNPs on GO with a mean size of 5.2 ± 0.2 nm via H_2 reduction of $HAuCl_4$ and GO, even though some aggregates of AuNPs were also seen.[92] Tang's group developed a "clean" method to grow Au and other metal (Pt, Pd) nanoclusters with an average diameter of 1.8 nm on RGO using sonication without any additional surfactants (Fig. 4).[93] The tunable reduction of GO sheets by adding various amounts of hydrazine was the key to give the possibility for the reduction of AuNCs by sonication. A similar result was reported that single-walled carbon nanotubes (SWNTs) could reduce $HAuCl_4$ to generate 7 nm AuNPs in the absence of additional reductants.[94]

2.3. Soft nitriding method

Although numerous efforts have been devoted to decorating ultrafine metal NPs on carbon supports, the weak interaction between noble metals and the carbon surface is still problematic. This may lead to the leaching of metal NPs in the catalytic process, resulting in the loss of catalytic performance. According to previous studies, through doping electron-rich heteroatoms like N,[95,96] P,[97,98] and S[99] elements into carbon nanomaterials, the electronic characteristics can be altered, thus producing more active sites and unexpected electrical and catalytic properties, such as high stability.[100] Zhang et al. proposed the synthesis of nanoporous carbon materials derived from glucose with N-containing additives by the hydrothermal carbonization (HTC) process, which were used as supports to confine Pd NPs of 5.9 nm.[101] They indicated that the

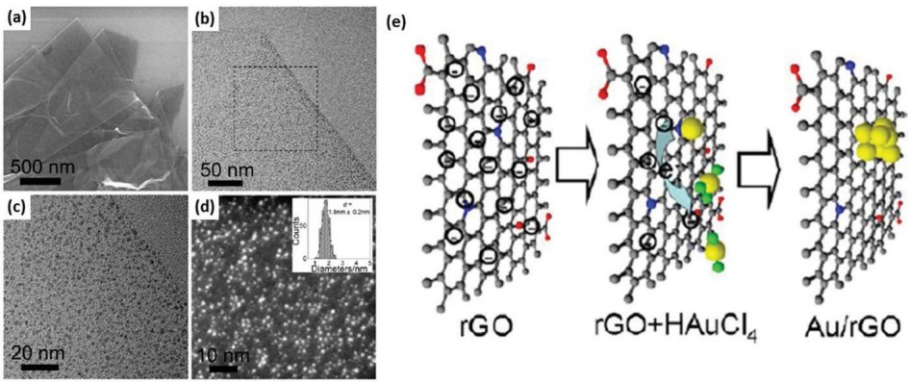

Fig. 4 Electron microscopy characterization of the as-synthesized Au/RGO (a–d). Scheme of the formation mechanism of Au/RGO hybrids (e). Reprinted (adapted) with permission from ref. 93. Copyright 2012, American Chemical Society.

incorporated N atoms into the carbon contributed to more structure defects which enhanced the adsorption of Pd. The interaction of surface N atoms and Pd also altered the electronic density of Pd species, which improved the reaction rate. A number of studies by Yin,[93] Koo[102] and Xie[103] showed that surface N atoms embedded in GO could act as initial nucleation sites for metal NPs. Nitrided carbon materials not only serve as reducing agents for metal precursors, but also increase the number of anchoring force to adsorb metal ions and NPs.

Recently, in situ growth of ligand-free ultrasmall (<2 nm) noble metal nanoclusters (e.g., Au, Pd and Pt) onto carbon supports was developed by our group (Fig. 5).[104-106] N-Doped carbon supports with abundant nitrogen sites were synthesized by annealing with urea at 300 °C. Urea decomposed into NH_3 and HCNO, effi cient to integrate surface N atoms on nearly any commercial carbon. In our synthesis, the surface N content can reach 19 at% in the form of pyridine/graphitic N into the graphene framework and ureido groups on the surface of carbon, respectively. The presence of these surface N species enhanced the affinity to metal ions and prevented the aggregation or overgrowth of Au. AuNCs of 1.6 nm with narrow size distribution were synthesized on the surface of nitrided carbon (denoted as AuNCs@NC) through a rapid chemical reduction of $HAuCl_4$ with $NaBH_4$. Moreover, the generality of the soft nitriding was confirmed using seven dff erent carbonaceous supports where the growth of AuNCs was independent of the initial properties of carbon supports. For the soft nitriding method, the size of AuNCs can be readily tuned by the pH of the solution. Larger AuNPs with an average diameter of 6-10 nm were grown at pH < 4 or >10. The faster nucleation of $AuCl_4^-$ occurred at lower pH. AuNCs nucleated and grew in aqueous solution rather than on the carbon surface at pH < 4. At pH > 10, the insuffi cient affinity of $AuCl_4^-$ to the carbon led to the overgrowth of AuNPs.

More recently, we extended this synthetic method to grow Au-Pd alloy NPs on nitrided carbon using AuNCs@NC as seeds (Fig. 6a and b).[107] When employing ascorbic acid and 4-mercaptobenzoic acid (4-MBA) as a mild reductant and surfactant, respectively, Au-Pd core-shell NPs (2-5 nm) with dff erent compositions of Au and Pd formed firstly (Fig. 6c-f), and then converted to Au-Pd alloy NPs after thermal activation at 250 °C for 1 h. The size of Au-Pd alloy NPs is uniform and highly controllable depending on the amount of the second precursors during the growth of the shell. Remarkably, the Au-Pd alloy NPs retained the uniform size without any aggregation or sintering after calcination. This confirms the strong affi nity of Au-Pd alloy NPs on the nitrided carbon support.

3. Electrocatalytic properties of Au@C nanocatalysts

3.1. Catalytic oxidation of methanol

Methanol as a feedstock for direct methanol fuel cells (DMFCs) is promising for clean energy technology alternative to fossil fuels. DMFCs have higher energy density and less pollutant/byproducts when using new anode catalysts.[108,109] The complete methanol oxidation reaction (MOR) involves six electrons and one water molecule or adsorbed residue (adsorbed OH^-), as follows:[110]

$$CH_3OH + H_2O \rightarrow CO_2 + 6H_{aq}^+ + 6e^- \quad (1)$$

However, the six-electron reaction is slow and relatively complex, involving the formation of several accumulated inter-

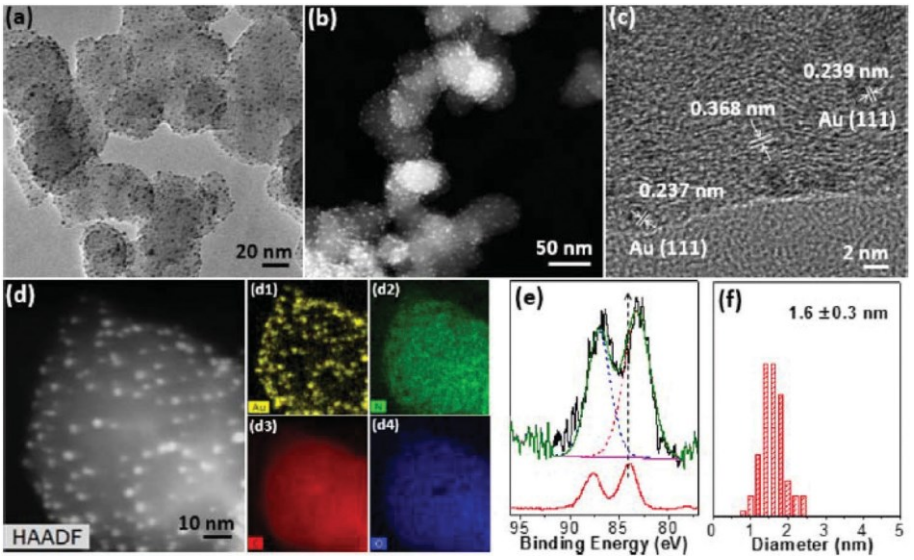

Fig. 5 Morphology characterization of AuNCs@NC: (a) bright-field TEM; (b) high-angle annular dark-field scanning TEM (HAADF-STEM); (c) high-resolution TEM images and (d) scanning TEM-energy dispersive X-ray spectroscopy mappings of AuNCs@NC: Au, N, C, and O are given in (d1–d4), respectively; (e) high-resolution X-ray photoelectron spectrum (XPS): Au 4f spectra of AuNCs@NC (top) and Au thin film (bottom); (f) the average diameter and distribution of AuNCs. Reprinted with permission from ref. 104. Copyright 2016, American Chemical Society.

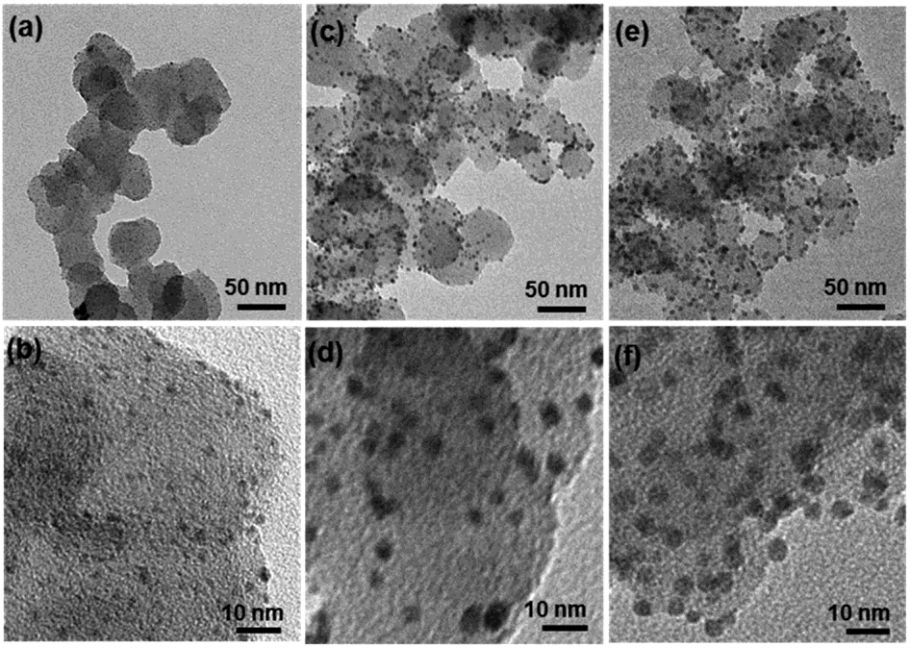

Fig. 6 Representative TEM images of Au-2@NC (a, b), Au@Au-5@NC (c, d) and Au@Pd-5@NC (e, f). Reprinted (adapted) with permission from ref. 107. Copyright 2018, Elsevier.

mediates such as CO, formaldehyde and formic acid other than CO_2 as the final product. The default highly efficient anode catalysts are Pt and Pt-based nanomaterials. However, these Pt-containing anode catalysts are expensive and susceptible to poisons like adsorbed CO and acid intermediates that potentially cause a fast decay in activity. These factors largely limit the lifetime and overall cost of DMFCs.

Being strongly resistant to the adsorption of CO-like intermediates, the reactivity of Au catalysts has attracted great attention in the applications of DMFCs, especially in alkaline media.[111-113] Several studies have suggested that AuNPs are excellent anode catalysts for electrocatalytic MOR.[114-117] Previous literature suggests that the MOR pathway catalyzed by Au is independent in two potential regions.[118,119] At lower potentials before the formation of an Au oxide layer, the chemical adsorption of OH^- and the possible preoxidation of the Au surface occur. Methanol is mainly oxidized to formates with four-electron exchange, as given below:[115,120]

$$CH_3OH + 5OH^- \rightarrow HCOO^- + 4H_2O + 4e^- \quad (2)$$

At higher potentials, the surface gold oxide monolayer restrains the chemiadsorption of OH^-, thus inhibiting the formation of formates. Methanol is oxidized to carbonates with six electrons directly, as given below:[104,107]

$$CH_3OH + 8OH^- \rightarrow CO_3^{2-} + 6H_2O + 6e^- \quad (3)$$

A typical example is the demonstration of methanol electrooxidation by AuNPs supported on activated carbon (6.7 nm) by Yan et al.[85] The synthesis was described in Section 2.2. AuNPs stabilized with PVP showed high activity for MOR in 0.1 M KOH with 5 M CH_3OH, reaching 48.6 mA mg_{Au}^{-1} at 0.355 V vs. Hg/HgO (Fig. 7a and b). In the low potential range (0.025–0.4 V), the catalytic activity of Au@C depended on the amount of adsorbed OH^- anions ($OH^-_{a\text{-}ads}$), thus the onset potential of the MOR shifted negatively with the increasing concentration of methanol and/or KOH (Fig. 7c and d). Yan and coworkers proposed that the $OH^-_{a\text{-}ads}$ species were beneficial to the acceleration of the reaction rate on the Au@C catalysts. The hydrogen-bonding interaction between adsorbed OH^- and methanol was suggested as the rate-determining step, as depicted below:

$$CH_3OH + OH^-_{a\text{-}ads} \rightarrow CH_2OH + H_2O + e^- \quad (4)$$

Subsequently, the same group further investigated the effect of the size and loading amount of AuNPs on MORs. They suggested that a better activity was obtained on smaller AuNPs with more active sites on the corners and edges.[121]

Given the slower mass and electron transfer caused by surface ligands and the unique size-dependent catalytic activity of Au, our group demonstrated the efficient oxidation of methanol using ligand-free ultrasmall AuNCs (1.6 ± 0.3 nm) supported on nitrided carbon.[104] The mass activity (current normalized to unit mass) was 1.2 A mg_{Au}^{-1} for AuNCs@NC at 1.11 V vs. RHE comparable to 1.9 A mg_{Pd}^{-1} at 0.8 V vs. RHE for Pd nanoclusters supported on nitrided carbon (Fig. 8a and c). The ultrasmall AuNCs expectedly exhibited much higher electroactivity compared to Au-6 nm@NC (obtained at pH 3). In the absence of surface ligands or surfactants, a low charge transfer resistance (1291 Ω) and a fast electron transfer rate (~0.02 cm s^{-1}) for ligand-free AuNCs@NC were revealed as shown in Fig. 8b. Ligand-free AuNCs@NC was threefold more

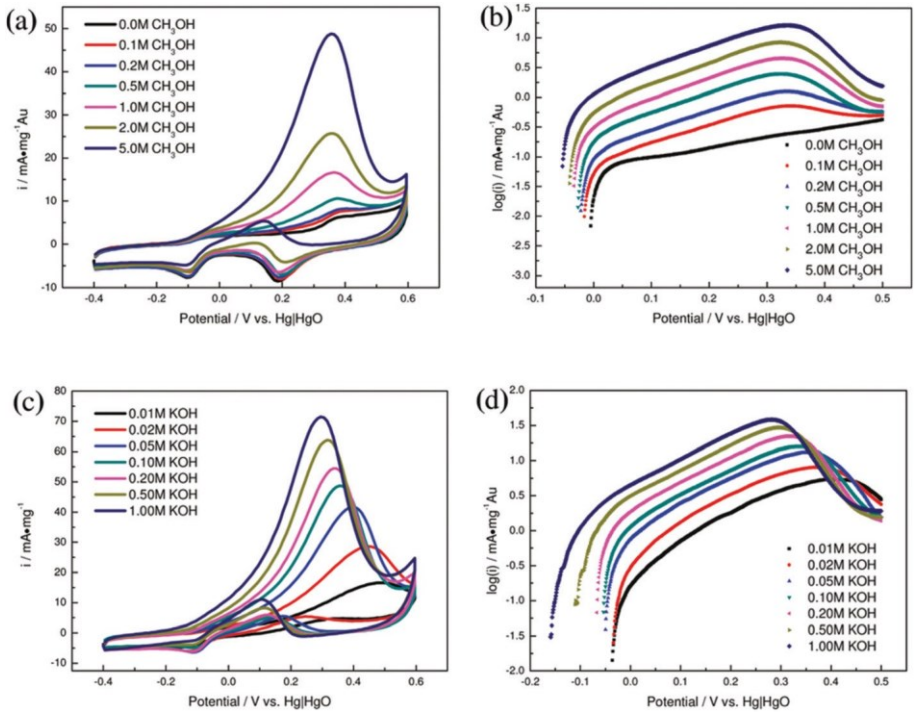

Fig. 7 Electrocatalytic oxidation of methanol in deoxygenated KOH solution: (a) cyclic voltammograms (CVs) on the Au@C nanocatalyst in 0.1 M KOH with different concentrations of methanol; (b) Tafel plots for electrooxidation of methanol on the Au@C nanocatalyst as a function of methanol concentration; (c) CVs on the Au@C nanocatalyst in deoxygenated 5 M CH_3OH with different concentrations of KOH solution; (d) Tafel plots for electrooxidation of methanol on the Au@C nanocatalyst as a function of KOH concentration. Reprinted with permission from ref. 85. Copyright 2011, American Chemical Society.

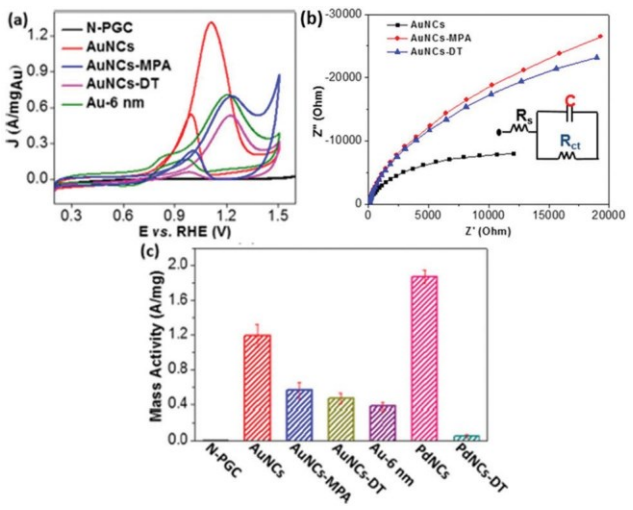

Fig. 8 Electrocatalytic oxidation of methanol using AuNCs@NC: (a) CVs of the NC, AuNCs@NC, AuNCs@NC-MPA, AuNCs@NC-DT and Au-6 nm@NC in 0.1 M NaOH with 1 M methanol; (b) electrochemical impedance spectroscopy (EIS) behaviors of different nanocatalysts to MOR with a frequency range from 0.1 to 100 000 Hz. The inset is the best fitted circuit diagram; (c) mass activities of different nanocatalysts at the peak potentials. Reprinted (adapted) with permission from ref. 104. Copyright 2016, American Chemical Society.

active than AuNCs@NC capped with 3-mercaptopropionic acid (MPA) and dodecanethiol (DT).

Although Au exhibits excellent resistance to the poisonous species, the activity of monometallic Au towards the MOR is lower compared to Pt-based nanocatalysts. The oxidation potential of methanol on Au nanocatalysts is 0.3 V higher than that on Pt catalysts. Alloying Pt or Pd with Au is a promising strategy to attain a superior activity accompanied by the anti-poisoning capacity. Zeng et al. designed the synthesis of core-shell Au-Pt NPs loaded on carbon which were used to catalyze the MOR in acidic media.[112] The electron exchange between the Au core and thin Pt shell played an important role in promoting the formation of active oxygen species on Pt, thus facilitating the removal of the accumulated carbonaceous intermediates. AuPt and AuPd nanoalloys dispersed on Vulcan XC-72 carbon also gave an excellent MOR activity with long-term stability as demonstrated by Hu[32] and Lu.[122,123]

3.2. Catalytic oxidation of ethanol and other alcohols

Although DMFCs have been developed for many decades, there are some disadvantages using methanol for fuel cells, e.g. toxicity of methanol, non-renewable sources and high methanol cross-over through membranes. As attractive alternatives, ethanol and other less toxic alcohols easily produced in large quantities from biomass have been considered lately.[110,124,125] The oxidation of ethanol is much more

complex. Twelve electrons are involved in the complete oxidation of ethanol, leading to sluggish reaction kinetics and numerous carbonaceous intermediates, as depicted below:

$$CH_3CH_2OH + 3H_2O \rightarrow 2CO_2 + 12H_{aq}^{+} + 12e^{-} \quad (5)$$

The generally studied reaction route is that ethanol is oxidized to acetate/acetic acid through four-electron oxidation in alkaline media, as given below:[126,127]

$$CH_3CH_2OH + 5OH^{-} \rightarrow CH_3COO^{-} + 4H_2O + 4e^{-} \quad (6)$$

It usually involves four consecutive steps on metal@C catalysts where the rate determining step is depicted in eqn (8) similar to the MOR.[128,129]

$$M + OH^{-} \rightarrow M - OH_{ads} + e^{-} \quad (7)$$

$$M\text{-}(CH_3CH_2OH)_{ads} + 3OH^{-} \rightarrow M\text{-}(COCH_3)_{ads} + 3H_2O + 3e^{-} \quad (8)$$

$$M\text{-}(COCH_3)_{ads} + M\text{-}OH_{ads} \rightarrow M\text{-}CH_3COOH + M \quad (9)$$

$$M\text{-}CH_3COOH + OH^{-} \rightarrow M + CH_3COO^{-} + H_2O \quad (10)$$

The nanostructured AuNPs are shown to be catalytically active in ethanol oxidation.[130,131] For instance, Yang et al. developed a rapid, template-free methodology to prepare hierarchical nanostructured Au nanoflowers (AuNFs) on carbon fiber cloth (CFC) via potentiostatic electrodeposition.[132] The open channels on the CFC support enabled the even distribution of AuNFs and efficient mass transport. The results of the ethanol electrooxidation reaction (EOR) showed that AuNFs exhibited 4 times higher catalytic activity and much less poisoning in contrast to AuNPs and bare gold electrodes. These features can be ascribed to their unique nanostructures such as the sharp edges or tips, which produced a larger surface area and more active sites. The size and shape driven activity of Au nanocatalysts in various electrochemical reactions including the oxidation of organic molecules, CO oxidation and oxygen reductions was also reported by Jena,[133] Qin,[134] and Li.[135]

Another example of alcohol electrooxidation on Au@C nanocatalysts was demonstrated by Yan et al. They used PVP-capped AuNPs supported on activated carbon to electrooxidize methanol, ethanol and ethylene glycol.[136] The mass-specific current densities on AuNPs peaked at 442 mA mg_{Au}^{-1} at 0.35 V vs. Hg/HgO in 0.1 M KOH solution with 2 M ethanol. In addition, unlike methanol and ethanol where the alcohol concentration influenced the mass activity, the mass activity of Au@C nanocatalysts was almost independent of the ethylene glycol concentration (Fig. 9a). However, the steady-state current densities of alcohols after 4000 s maintained ~40% of the initial (Fig. 9b). The incorporation of heteroatoms into the carbon frameworks or doping metals with non-metal elements has emerged as an effective strategy to enhance the interactions between AuNPs and supports. Recently, Li et al. synthesized a series of carbon supported Au-phosphorus (AuP@C) catalysts by a hot-reflux method using white phosphorus (P_4) as a reductant and a dopant.[137] The mass activity of AuP@C (3.7 nm) was 7.83-fold higher than that of the undoped Au@C

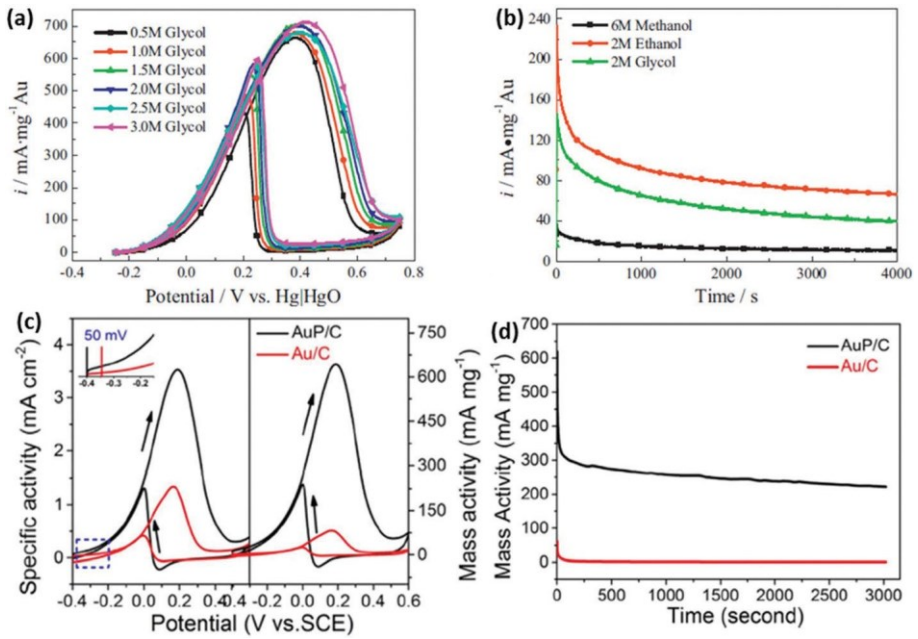

Fig. 9 (a) CVs on the Au@C catalyst in deoxygenated 0.1 M KOH solution with different concentrations of ethylene glycol; (b) chronoamperograms on the Au@C catalyst in deoxygenated 0.1 M KOH solution at the potential of 0.25 V vs. Hg/HgO with different alcohols. Adapted with permission from ref. 136. Copyright 2013, Elsevier; (c) mass and specific normalized CVs and (d) chronoamperometry curves of the AuP@C and Au@C catalysts in N_2-saturated 0.5 M KOH and 1.0 M C_2H_5OH mixing solutions at a potential of 0.20 V vs. SCE. Adapted with permission from ref. 137. Copyright 2017, Elsevier.

(5.6 nm) prepared by $NaBH_4$ reduction (Fig. 9c). This is attributed to the highly uniform distribution of ultrafine AuP NPs and the altered electronic structure of Au by interaction with P. The initial oxidation potential of the EOR on the AuP@C nanocatalyst shifted negatively about 50 mV compared to that of the Au@C catalyst, indicating better electrocatalytic performance at a lower potential. The lower d-band center caused by P doping further weakened the adsorption of the intermediates on the Au surface, thus enhancing the poisoning resistance and attaining a relatively high steady-state current density in comparison with the Au@C catalyst as shown in Fig. 9d. This further verified that the AuP@C catalyst displayed a better stability for ethanol oxidation.

Considering the synergetic effects between the two components of bimetallic NPs, there are a number of reports on supported Au-bimetallic NPs for EOR catalysis.[138-140] Our group confirmed that the synergy between Au and Pd could effectively enhance long-time stability and accelerate charge transfer in comparison with monometallic NPs.[107] In our recent work, the specific activity of AuPd NPs supported on nitrided carbon (AuPd NPs@NC) was approximately 5 times more than commercial Pd/C (5 wt% loading) when the Au/Pd ratio was 45 : 55. Moreover, the chronoamperometric response showed that the current decay for AuPd NPs@NC (45 : 55) was much slower and maintained the highest steady-state current density, 2.9 times higher than that of commercial Pd/C, which indicated that alloying Au with Pd not only enhanced the electrocatalytic activity, but also improved the stability of catalysts. Additionally, alloying with a small amount of Au (10%) significantly enhanced the oxidation current density and resulted in the highest peak current density ratio (I_f/I_b) of the forward (I_f) to the backward scan (I_b) up to 5.8 compared to all other catalysts with different compositions of Au and Pd, indicating the improved poisoning tolerance by the introduction of Au into Pd.

3.3. Oxidation of guanines in DNA and amines

The guanine (G) and adenine (A) bases in the DNA molecular skeleton are easy to electrooxidize.[141-143] A single electron oxidation potential of G and A bases is higher than +1.2 V vs. NHE and the oxidation of cytosine (C) and thymine (T) bases requires a higher potential.[144,145] The detection of DNA or DNA damage by the direct oxidation current of nucleic acid bases can reach the sensitivity of nanomoles.[146] However, the electrochemical oxidation of electrodes and/or decomposition of solvent molecules (e.g., water) is often caused by the positive base oxidation potential during testing, thus resulting in a very high background current and interfering with the DNA oxidation signals. The common method is to use indirect electrochemical signal conversion through charge mediators. For instance, when coupling $Ru(bpy)_3^{2+}$ with DNA molecules on the electrode surface, the redox reaction of Ru^{2+} can mediate the oxidation of guanine. This method has little effect on the electrolytic background current of water and the non-specific adsorption of the target DNA molecule. The electrochemical detection of the label-free target DNA molecule was successfully achieved.[147] On the other hand, tripropylamine (TprA) is an important trialkylamine as an efficient co-reactant for electrochemiluminescence (ECL) in biosensor technology.[148] Since the electrochemical oxidation of TprA occurs at about +0.85 V (vs. Ag/AgCl), the oxidation of TprA is a useful probe to examine the oxidative damage of biomolecules during detection sequence or DNA analysis.[149]

As reported by our group recently, the AuNCs@NC catalysts were incorporated into films of architecture {poly(diallyldimethylammonium) (PDDA)/AuNCs@NC}$_n$ by using layer-by-layer (LBL) assembly with oppositely charged PDDA on pyrolytic graphite (PG) electrodes for the electrocatalytic oxidation of double-stranded (ds)-DNA and TprA.[105] Ligand-free AuNCs@NC in these films exhibited excellent electrocatalytic oxidation activity for ds-DNA and TprA. The oxidation peak potential of DNA showed a negative shift by 140 mV and the peak current was enhanced by three times on the {PDDA/AuNCs@NC}$_2$/PDDA film electrode compared to the blank electrode (Fig. 10A). Similarly, the oxidation peak current density of TprA on the {PDDA/AuNCs@NC}$_3$ film electrode increased dramatically to 4.7 A mg_{Au}^{-1} with a negative shift (~200 mV) of the peak potential compared to the control films (without AuNCs) (Fig. 10B). Meanwhile, 86% of catalytic current was still retained after 100 scanning cycles, and the resulting {PDDA/AuNCs@NC}$_3$ film displayed a superior stability. A strong electrochemical response of DNA adsorbed on AuNPs is usually difficult to observe and measure due to the overlap with the Au oxidation peak.[150,151] However, in our case, the highly dispersed ligand-free ultrasmall AuNCs exhibited a lower oxidation potential and an unexpected capacity for amplifying the detection signal. The supported AuNCs may provide a promising approach for practical applications in biotechnology.

The research work mentioned in the third section is summarized in Table 2. Various Au@C nanocatalysts exhibited excellent electrocatalytic performance for methanol, ethanol, TprA and guanines in DNA molecules. Among these nanocatalysts, AuNCs@NC exhibited superior mass activity (1190 mA mg_{Au}^{-1}) and AuP@C had the highest specific activity (3.53 mA cm^{-2}) toward the MOR and EOR, respectively.[104,137] Ligand-free

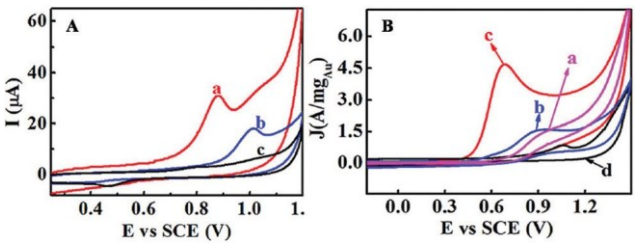

Fig. 10 (A) CVs of the {PDDA/AuNCs@NC}$_2$/PDDA/DNA (a), {PDDA/NC}$_2$/PDDA/DNA (b) and {PDDA/AuNCs@NC}$_2$ (c) electrodes in 0.01 M phosphate buffers, pH 7.4; (B) CVs of the bare PG (a), {PDDA/NC}$_3$ (b), {PDDA/AuNCs@NC}$_3$ (c) electrodes in 0.01 M TprA solution, and {PDDA/AuNCs@NC}$_3$ electrode (d) in the absence of 0.01 M TprA. Adapted with permission from ref. 105. Copyright 2016, John Wiley and Sons.

Table 2 Electrocatalytic performances of Au@C nanocatalysts for methanol, ethanol, guanines in DNA and TprA oxidation reaction

Catalyst composition	Preparation method	Average diameter (nm)	Catalytic reaction	Mass activity (mA mg^{-1})	Specific activity (mA cm^{-2})	I_f/I_b	Ref.
PtAu@graphene	Electrodeposition	150-200	MOR	394	—	1.25	32
Au@C	Rapid reduction	6.7	MOR	48.6	—	—	85
AuNCs@NC	Soft nitriding	0.7-2	MOR	1190	—	—	104
AuPt NPs@C	Seed-mediated growth	4-10	MOR	—	1.65	—	112
Au@C[a]	Rapid reduction	4.73	MOR	47.06	—	—	121
Au_2Pt_1@C	Capping agent-free	3.4	MOR	—	—	1.84	122
Pd_2Au@GC[b]	Hydrothermal	11.42	MOR	491.84	1.09	—	123
AuPd NPs@NC	Seed-mediated growth	2-5	EOR	430	1.11	5.8	107
Au NFs[c]@CFC[d]	Electrodeposition	—	EOR	—	—	0.29	132
AuNPs@C	Deposition reduction	4.65	MOR, EOR	69.5 (MOR), 442 (EOR)	—	—	136
AuP@C	Hot-reflux	3.7	EOR	642.33	3.53	—	137
AuNCs@NC	Soft nitriding	1.6	guanines and TprA	—	—	—	105

[a] Au@C catalyst with 20 wt% Au. [b] GC: glassy carbon. [c] NFs: nanoflowers. [d] CFC: carbon fiber cloth.

AuNCs@NC assembled in $\{PDDA/AuNCs@N\text{-}C\}_n$ films exhibited unexpected activity for electrooxidation of guanines in DNA and TprA with reduced oxidation potentials. This makes it possible to facilitate their application in biosensors.[105]

4. Outlook

We summarized the most recent studies on Au nanocatalysts supported on conductive carbon as anode catalysts for electrooxidation of alcohols, guanines in DNA and TprA. Au as a chemically stable catalyst shows unique size-dependent catalytic properties. Although numerous efforts have been devoted to designing Au@C nanocomposites, there are still unmet challenges in the synthesis and application of Au@C as catalysts. One of the obvious problems in the use of Au@C is the cost of catalysts, since Au is as expensive as Pt. The apparent solution is to decrease the size of AuNPs that potentially exposes more surface atoms for catalysis. However, due to the large surface energy, the stabilization of these AuNPs on carbon supports has become critical. The new methods for surface modification and functionalization of carbon by integrating heteroatoms as binding sites of AuNPs should be further investigated for low cost and scale up production. Other carbon supports such as mesoporous carbon, and MOF-derived nanomaterials can potentially be used for Au@C to offer a high surface area and adjustable pore size, as well as to restrain the overgrowth of Au nanostructures during the synthesis. Using carbon with a high N content, it is possible to prepare a single-atom Au catalyst where atomic Au can be well dispersed and stabilized through the coordination of multiple N atoms.[152] It will be of interest to study the electrocatalytic performance of single-atom Au catalysts since the atom efficiency of Au can reach 100%.

Understanding the electronic interaction between Au and doped carbon is an attractive alternative to develop Au@C as highly selective catalysts for heterogeneous reactions. Through changing the surface electron density of AuNPs, Au has been used to catalyze selective hydrogenation of C=C bonds[153] and oxidation of C=C bonds.[106] Heteroatoms, like N and P, can induce electronic perturbation at the Au-carbon interface, where the catalytic selectivity usually relies on. The electron-rich Au nanocatalysts also tend to favor the binding of electrophiles, like CO_2, to promote the reaction selectivity.

Other than the electronic interactions of Au and doped carbon, surface ligands can potentially modulate the reaction pathway as well.[154] Unlike surface ligands with long alkyl chains which block the electron transfer, short ligands can potentially play a critical role in electrocatalysis. Chang and Yang demonstrated that N-heterocyclic carbene-functionalized AuNPs selectively reduced CO_2 to CO with a faradaic efficiency of 83%, since carbene showed a strong σ-donation with AuNPs.[155] More attention on the use of carbon supports and surface ligands as a means to control the surface electronic properties of Au nanocatalysts should be given in future studies.

Conflicts of interest

The authors declare no competing financial interest.

Acknowledgements

J. F. R. is grateful for the financial support from the National Institute of Environmental Health Sciences (NIH, Grant No. ES03154). J. H. acknowledges the support from the National Science Foundation (CBET 1705566). Z. C. acknowledges the support from the China Scholarship Council for her visiting at the University of Connecticut. Y. Y. acknowledges the support from the China Scholarship Council and Nanjing University of Science and Technology for her visiting at the University of Connecticut.

References

1 B. R. Cuenya, S.-H. Baeck, T. F. Jaramillo and E. W. McFarland, J. Am. Chem. Soc., 2003, 125, 12928-12934.

2 M.-C. Daniel and D. Astruc, Chem. Rev., 2004, 104, 293-346.
3 S. Panigrahi, S. Basu, S. Praharaj, S. Pande, S. Jana, A. Pal, S. K. Ghosh and T. Pal, J. Phys. Chem. C, 2007, 111, 4596-4605.
4 R. Sardar, A. M. Funston, P. Mulvaney and R. W. Murray, Langmuir, 2009, 25, 13840-13851.
5 M. Haruta, J. New Mater. Electrochem. Syst., 2004, 7, 163-172.
6 M. Haruta, T. Kobayashi, H. Sano and N. Yamada, Chem. Lett., 1987, 16, 405-408.
7 M. Haruta, N. Yamada, T. Kobayashi and S. Iijima, J. Catal., 1989, 115, 301-309.
8 H. Sakurai, S. Tsubota and M. Haruta, Appl. Catal., A, 1993, 102, 125-136.
9 H. Sakurai and M. Haruta, Catal. Today, 1996, 29, 361-365.
10 A. Ueda, T. Oshima and M. Haruta, Appl. Catal., B, 1997, 12, 81-93.
11 B. Uphade, S. Tsubota, T. Hayashi and M. Haruta, Chem. Lett., 1998, 27, 1277-1278.
12 M. Haruta, CATTECH, 2002, 6, 102-115.
13 C. Ma, W. Xue, J. Li, W. Xing and Z. Hao, Green Chem., 2013, 15, 1035-1041.
14 H. Abroshan, G. Li, J. Lin, H. J. Kim and R. Jin, J. Catal., 2016, 337, 72-79.
15 J. B. Zhao and R. C. Jin, Nano Today, 2018, 18, 86-102.
16 M. Haruta, Catal. Today, 1997, 36, 153-166.
17 X. Y. Liu, A. Wang, T. Zhang and C.-Y. Mou, Nano Today, 2013, 8, 403-416.
18 M. Comotti, W.-C. Li, B. Spliethoff and F. Schüth, J. Am. Chem. Soc., 2006, 128, 917-924.
19 X. Nie, H. Qian, Q. Ge, H. Xu and R. Jin, ACS Nano, 2012, 6, 6014-6022.
20 W. Yan, S. M. Mahurin, Z. Pan, S. H. Overbury and S. Dai, J. Am. Chem. Soc., 2005, 127, 10480-10481.
21 X. Liu, M.-H. Liu, Y.-C. Luo, C.-Y. Mou, S. D. Lin, H. Cheng, J.-M. Chen, J.-F. Lee and T.-S. Lin, J. Am. Chem. Soc., 2012, 134, 10251-10258.
22 Q. Yue, Y. Zhang, C. Wang, X. Wang, Z. Sun, X.-F. Hou, D. Zhao and Y. Deng, J. Mater. Chem. A, 2015, 3, 4586-4594.
23 T. Zeng, X.-L. Zhang, H.-Y. Niu, Y.-Y. Ma, W.-H. Li and Y.-Q. Cai, Appl. Catal., B, 2013, 134–135, 26-33.
24 S. Miao, C. Zhang, Z. Liu, B. Han, Y. Xie, S. Ding and Z. Yang, J. Phys. Chem. C, 2008, 112, 774-780.
25 J. Han, Y. Liu, L. Li and R. Guo, Langmuir, 2009, 25, 11054-11060.
26 J. Han, L. Li and R. Guo, Macromolecules, 2010, 43, 10636-10644.
27 A. Villa, M. Schiavoni and L. Prati, Catal. Sci. Technol., 2012, 2, 673-682.
28 M. Rocha, C. Fernandes, C. Pereira, S. L. H. Rebelo, M. F. R. Pereira and C. Freire, RSC Adv., 2015, 5, 5131-5141.
29 X. Ma, X. Li, N. Lun and S. Wen, Mater. Chem. Phys., 2006, 97, 351-356.
30 M. Simões, S. Baranton and C. Coutanceau, J. Phys. Chem. C, 2009, 113, 13369-13376.
31 Z. Dong, X. Le, Y. Liu, C. Dong and J. Ma, J. Mater. Chem. A, 2014, 2, 18775-18785.
32 Y. Hu, H. Zhang, P. Wu, H. Zhang, B. Zhou and C. Cai, Phys. Chem. Chem. Phys., 2011, 13, 4083-4094.
33 M. Yang, M. Zhou, A. Zhang and C. Zhang, J. Phys. Chem. C, 2012, 116, 22336-22340.
34 S. Demirel, P. Kern, M. Lucas and P. Claus, Catal. Today, 2007, 122, 292-300.
35 T. Benkó, A. Beck, O. Geszti, R. Katona, A. Tungler, K. Frey, L. Guczi and Z. Schay, Appl. Catal., A, 2010, 388, 31-36.
36 B. Fang, M. Kim and J.-S. Yu, Appl. Catal., B, 2008, 84, 100-105.
37 J. H. Bang, Electrochim. Acta, 2011, 56, 8674-8679.
38 J. Planeix, N. Coustel, B. Coq, V. Brotons, P. Kumbhar, R. Dutartre, P. Geneste, P. Bernier and P. Ajayan, J. Am. Chem. Soc., 1994, 116, 7935-7936.
39 G. L. Bezemer, J. H. Bitter, H. P. Kuipers, H. Oosterbeek, J. E. Holewijn, X. Xu, F. Kapteijn, A. J. van Dillen and K. P. de Jong, J. Am. Chem. Soc., 2006, 128, 3956-3964.
40 T. Xue, S. Jiang, Y. Qu, Q. Su, R. Cheng, S. Dubin, C. Y. Chiu, R. Kaner, Y. Huang and X. Duan, Angew. Chem., 2012, 124, 3888-3891.
41 B. Liu, H.-Q. Yao, R. A. Daniels, W.-Q. Song, H.-Q. Zheng, L. Jin, S. L. Suib and J. He, Nanoscale, 2016, 8, 5441-5445.
42 B. Liu, L. Jin, H.-Q. Zheng, H.-Q. Yao, Y. Wu, A. Lopes and J. He, ACS Appl. Mater. Interfaces, 2017, 9, 1746-1758.
43 W. Chaikittisilp, K. Ariga and Y. Yamauchi, J. Mater. Chem. A, 2013, 1, 14-19.
44 L. Prati and M. Rossi, J. Catal., 1998, 176, 552-560.
45 J. L. Figueiredo, J. Mater. Chem. A, 2013, 1, 9351-9364.
46 Z. Ma and S. Dai, Nano Res., 2011, 4, 3-32.
47 L. Jin, B. Liu, P. Wang, H. Q. Yao, L. Achola, P. Kerns, A. Lopes, Y. Yang, J. Ho, A. Moewes, Y. Pei and J. He, Nanoscale, 2018, DOI: 10.1039/C8NR04322A.
48 Y. Xu, L. Chen, X. Wang, W. Yao and Q. Zhang, Nanoscale, 2015, 7, 10559-10583.
49 A. Wang, X. Y. Liu, C.-Y. Mou and T. Zhang, J. Catal., 2013, 308, 258-271.
50 J. Zhao, T. Zhang, X. Di, J. Xu, J. Xu, F. Feng, J. Ni and X. Li, RSC Adv., 2015, 5, 6925-6931.
51 I. B. Gallo, E. A. Carbonio and H. M. Villullas, ACS Catal., 2018, 8, 1818-1827.
52 L. Kesavan, R. Tiruvalam, M. H. Ab Rahim, M. I. bin Saiman, D. I. Enache, R. L. Jenkins, N. Dimitratos, J. A. Lopez-Sanchez, S. H. Taylor and D. W. Knight, Science, 2011, 331, 195-199.
53 P. Raghavendra, G. Vishwakshan Reddy, R. Sivasubramanian, P. Sri Chandana and L. Subramanyam Sarma, Int. J. Hydrogen Energy, 2018, 43, 4125-4135.
54 T. Schmidt, Z. Jusys, H. Gasteiger, R. Behm, U. Endruschat and H. Boennemann, J. Electroanal. Chem., 2001, 501, 132-140.

55 S. Xie, H. Tsunoyama, W. Kurashige, Y. Negishi and T. Tsukuda, ACS Catal., 2012, 2, 1519-1523.
56 L. Lu, Y. Nie, Y. Wang, G. Wu, L. Li, J. Li, X. Qi and Z. Wei, J. Mater. Chem. A, 2018, 6, 104-109.
57 G. Selvarani, S. V. Selvaganesh, S. Krishnamurthy, G. Kiruthika, P. Sridhar, S. Pitchumani and A. Shukla, J. Phys. Chem. C, 2009, 113, 7461-7468.
58 Q. He, W. Chen, S. Mukerjee, S. Chen and F. Laufek, J. Power Sources, 2009, 187, 298-304.
59 J. Mathiyarasu and K. L. N. Phani, J. Electrochem. Soc., 2007, 154, B1100-B1105.
60 H. Zhang, B. Dai, W. Li, X. Wang, J. Zhang, M. Zhu and J. Gu, J. Catal., 2014, 316, 141-148.
61 A. Habrioux, W. Vogel, M. Guinel, L. Guetaz, K. Servat, B. Kokoh and N. Alonso-Vante, Phys. Chem. Chem. Phys., 2009, 11, 3573-3579.
62 L. D. Zhu, T. S. Zhao, J. B. Xu and Z. X. Liang, J. Power Sources, 2009, 187, 80-84.
63 C. Shang, W. Hong, J. Wang and E. Wang, J. Power Sources, 2015, 285, 12-15.
64 R. Cao, T. Xia, R. Zhu, Z. Liu, J. Guo, G. Chang, Z. Zhang, X. Liu and Y. He, Appl. Surf. Sci., 2018, 433, 840-846.
65 S. D. Lankiang, S. Baranton and C. Coutanceau, Electrochim. Acta, 2017, 242, 287-299.
66 Y. Lin, S. Taylor, H. Li, K. A. S. Fernando, L. Qu, W. Wang, L. Gu, B. Zhou and Y.-P. Sun, J. Mater. Chem., 2004, 14, 527-541.
67 W. Hong, H. Bai, Y. Xu, Z. Yao, Z. Gu and G. Shi, J. Phys. Chem. C, 2010, 114, 1822-1826.
68 J. Huang, L. Zhang, B. Chen, N. Ji, F. Chen, Y. Zhang and Z. Zhang, Nanoscale, 2010, 2, 2733-2738.
69 Q. Zhuo, Y. Ma, J. Gao, P. Zhang, Y. Xia, Y. Tian, X. Sun, J. Zhong and X. Sun, Inorg. Chem., 2013, 52, 3141-3147.
70 F. Li, H. Yang, C. Shan, Q. Zhang, D. Han, A. Ivaska and L. Niu, J. Mater. Chem., 2009, 19, 4022-4025.
71 B. Kim and W. M. Sigmund, Langmuir, 2004, 20, 8239-8242.
72 K. Jiang, A. Eitan, L. S. Schadler, P. M. Ajayan, R. W. Siegel, N. Grobert, M. Mayne, M. Reyes-Reyes, H. Terrones and M. Terrones, Nano Lett., 2003, 3, 275-277.
73 Y. Fang, S. Guo, C. Zhu, Y. Zhai and E. Wang, Langmuir, 2010, 26, 11277-11282.
74 M. Balcioglu, M. Rana and M. V. Yigit, J. Mater. Chem. B, 2013, 1, 6187-6193.
75 L. Han, W. Wu, F. L. Kirk, J. Luo, M. M. Maye, N. N. Kariuki, Y. Lin, C. Wang and C.-J. Zhong, Langmuir, 2004, 20, 6019-6025.
76 Y.-Y. Ou and M. H. Huang, J. Phys. Chem. B, 2006, 110, 2031-2036.
77 Y. Shi, R. Yang and P. K. Yuet, Carbon, 2009, 47, 1146-1151.
78 C. Han, L. Wu, L. Ge, Y. Li and Z. Zhao, Carbon, 2015, 92, 31-40.
79 S. Zhang, Y. Shao, H.-G. Liao, J. Liu, I. A. Aksay, G. Yin and Y. Lin, Chem. Mater., 2011, 23, 1079-1081.
80 V. K. Gupta, M. L. Yola, N. Atar, Z. Üstündağ and A. O. Solak, J. Mol. Liq., 2014, 191, 172-176.
81 V. K. Gupta, N. Atar, M. L. Yola, Z. Ustundag and L. Uzun, Water Res., 2014, 48, 210-217.
82 G. Goncalves, P. A. A. P. Marques, C. M. Granadeiro, H. I. S. Nogueira, M. K. Singh and J. Grácio, Chem. Mater., 2009, 21, 4796-4802.
83 R. Pocklanova, A. K. Rathi, M. B. Gawande, K. K. R. Datta, V. Ranc, K. Cepe, M. Petr, R. S. Varma, L. Kvitek and R. Zboril, J. Mater. Chem. A, 2016, 424, 121-127.
84 Z. Zhang, H. Chen, C. Xing, M. Guo, F. Xu, X. Wang, H. J. Gruber, B. Zhang and J. Tang, Nano Res., 2011, 4, 599-611.
85 S. Yan, S. Zhang, Y. Lin and G. Liu, J. Phys. Chem. C, 2011, 115, 6986-6993.
86 S. Peng, Y. Lee, C. Wang, H. Yin, S. Dai and S. Sun, Nano Res., 2008, 1, 229-234.
87 H. Tsunoyama, N. Ichikuni, H. Sakurai and T. Tsukuda, J. Am. Chem. Soc., 2009, 131, 7086-7093.
88 X. Huang, X. Zhou, S. Wu, Y. Wei, X. Qi, J. Zhang, F. Boey and H. Zhang, Small, 2010, 6, 513-516.
89 J. A. Lopez-Sanchez, N. Dimitratos, C. Hammond, G. L. Brett, L. Kesavan, S. White, P. Miedziak, R. Tiruvalam, R. L. Jenkins and A. F. Carley, Nat. Chem., 2011, 3, 551-556.
90 D. Li, C. Wang, D. Tripkovic, S. Sun, N. M. Markovic and V. R. Stamenkovic, ACS Catal., 2012, 2, 1358-1362.
91 L. Zhao, W. Gu, C. Zhang, X. Shi and Y. Xian, J. Colloid Interface Sci., 2016, 465, 279-285.
92 L. Shao, X. Huang, D. Teschner and W. Zhang, ACS Catal., 2014, 4, 2369-2373.
93 H. Yin, H. Tang, D. Wang, Y. Gao and Z. Tang, ACS Nano, 2012, 6, 8288-8297.
94 H. C. Choi, M. Shim, S. Bangsaruntip and H. Dai, J. Am. Chem. Soc., 2002, 124, 9058-9059.
95 K. Gong, F. Du, Z. Xia, M. Durstock and L. Dai, Science, 2009, 323, 760-764.
96 L. Qu, Y. Liu, J.-B. Baek and L. Dai, ACS Nano, 2010, 4, 1321-1326.
97 B. Liu, L. Jin, W. Zhong, A. Lopes, S. L. Suib and J. He, Chem. – Eur. J., 2018, 24, 2565-2569.
98 G. Hasegawa, T. Deguchi, K. Kanamori, Y. Kobayashi, H. Kageyama, T. Abe and K. Nakanishi, Chem. Mater., 2015, 27, 4703-4712.
99 X. Ji, K. T. Lee, R. Holden, L. Zhang, J. Zhang, G. A. Botton, M. Couillard and L. F. Nazar, Nat. Chem., 2010, 2, 286.
100 Y. Li, Y. Zhao, H. Cheng, Y. Hu, G. Shi, L. Dai and L. Qu, J. Am. Chem. Soc., 2011, 134, 15-18.
101 P. Zhang, Y. Gong, H. Li, Z. Chen and Y. Wang, Nat. Commun., 2013, 4, 1593.
102 H. Y. Koo, H.-J. Lee, Y.-Y. Noh, E.-S. Lee, Y.-H. Kim and W. San Choi, J. Mater. Chem., 2012, 22, 7130-7135.
103 X. Xie, J. Long, J. Xu, L. Chen, Y. Wang, Z. Zhang and X. Wang, RSC Adv., 2012, 2, 12438-12446.

104 B. Liu, H. Yao, W. Song, L. Jin, I. M. Mosa, J. F. Rusling, S. L. Suib and J. He, J. Am. Chem. Soc., 2016, 138, 4718-4721.
105 H. Yao, B. Liu, I. M. Mosa, I. Bist, J. He and J. F. Rusling, ChemElectroChem, 2016, 3, 2100-2109.
106 B. Liu, P. Wang, A. Lopes, L. Jin, W. Zhong, Y. Pei, S. L. Suib and J. He, ACS Catal., 2017, 7, 3483-3488.
107 Y. Yang, L. Jin, B. Liu, P. Kerns and J. He, Electrochim. Acta, 2018, 269, 441-451.
108 X. Ren, P. Zelenay, S. Thomas, J. Davey and S. Gottesfeld, J. Power Sources, 2000, 86, 111-116.
109 K. M. McGrath, G. S. Prakash and G. A. Olah, J. Ind. Eng. Chem., 2004, 10, 1063-1080.
110 C. Lamy, A. Lima, V. LeRhun, F. Delime, C. Coutanceau and J.-M. Léger, J. Power Sources, 2002, 105, 283-296.
111 K. Mikkelsen, B. Cassidy, N. Hofstetter, L. Bergquist, A. Taylor and D. A. Rider, Chem. Mater., 2014, 26, 6928-6940.
112 J. Zeng, J. Yang, J. Y. Lee and W. Zhou, J. Phys. Chem. B, 2006, 110, 24606-24611.
113 J. Luo, P. N. Njoki, Y. Lin, D. Mott, L. Wang and C.-J. Zhong, Langmuir, 2006, 22, 2892-2898.
114 M. Graf, M. Haensch, J. Carstens, G. Wittstock and J. Weissmüller, Nanoscale, 2017, 9, 17839-17848.
115 Z. Borkowska, A. Tymosiak-Zielinska and G. Shul, Electrochim. Acta, 2004, 49, 1209-1220.
116 J. Luo, V. W. Jones, M. M. Maye, L. Han, N. N. Kariuki and C.-J. Zhong, J. Am. Chem. Soc., 2002, 124, 13988-13989.
117 C.-J. Zhong and M. M. Maye, Adv. Mater., 2001, 13, 1507-1511.
118 M. Bełtowska-Brzezinska, T. Łuczak and R. Holze, J. Appl. Electrochem., 1997, 27, 999-1011.
119 K. Assiongbon and D. Roy, Surf. Sci., 2005, 594, 99-119.
120 J. Zhang, P. Liu, H. Ma and Y. Ding, J. Phys. Chem. C, 2007, 111, 10382-10388.
121 S. Yan and S. Zhang, Int. J. Hydrogen Energy, 2011, 36, 13392-13397.
122 L. Lu, Y. Nie, Y. Wang, G. Wu, L. Li, J. Li, X. Qi and Z. Wei, J. Mater. Chem. A, 2018, 6, 104-109.
123 L.-M. Luo, R.-H. Zhang, D. Chen, Q.-Y. Hu, X. Zhang, C.-Y. Yang and X.-W. Zhou, Electrochim. Acta, 2018, 259, 284-292.
124 H. R. Corti and E. R. Gonzalez, Direct alcohol fuel cells: materials, performance, durability and applications, Springer Science & Business Media, 2013.
125 M. Kamarudin, S. K. Kamarudin, M. Masdar and W. R. W. Daud, Int. J. Hydrogen Energy, 2013, 38, 9438-9453.
126 S. Shen, T. Zhao and Q. Wu, Int. J. Hydrogen Energy, 2012, 37, 575-582.
127 G. Tremiliosi-Filho, E. Gonzalez, A. Motheo, E. Belgsir, J.-M. Leger and C. Lamy, J. Electroanal. Chem., 1998, 444, 31-39.
128 C. Bianchini and P. K. Shen, Chem. Rev., 2009, 109, 4183-4206.
129 Z. Liang, T. Zhao, J. Xu and L. Zhu, Electrochim. Acta, 2009, 54, 2203-2208.
130 J.-J. Feng, A.-Q. Li, Z. Lei and A.-J. Wang, ACS Appl. Mater. Interfaces, 2012, 4, 2570-2576.
131 M. Stratakis and H. Garcia, Chem. Rev., 2012, 112, 4469-4506.
132 F. Yang, K. Cheng, K. Ye, X. Xiao, F. Guo, J. Yin, G. Wang and D. Cao, Electrochim. Acta, 2013, 114, 478-483.
133 B. K. Jena and C. R. Raj, Langmuir, 2007, 23, 4064-4070.
134 Y. Qin, Y. Song, N. Sun, N. Zhao, M. Li and L. Qi, Chem. Mater., 2008, 20, 3965-3972.
135 Y. Li and G. Shi, J. Phys. Chem. B, 2005, 109, 23787-23793.
136 S. Yan, L. Gao, S. Zhang, W. Zhang, Y. Li and L. Gao, Electrochim. Acta, 2013, 94, 159-164.
137 T. Li, G. Fu, J. Su, Y. Wang, Y. Lv, X. Zou, X. Zhu, L. Xu, D. Sun and Y. Tang, Electrochim. Acta, 2017, 231, 13-19.
138 Z.-L. Wang, J.-M. Yan, H.-L. Wang, Y. Ping and Q. Jiang, J. Mater. Chem. A, 2013, 1, 12721-12725.
139 Y.-Y. Feng, Z.-H. Liu, Y. Xu, P. Wang, W.-H. Wang and D.-S. Kong, J. Power Sources, 2013, 232, 99-105.
140 F. Ksar, L. Ramos, B. Keita, L. Nadjo, P. Beaunier and H. Remita, Chem. Mater., 2009, 21, 3677-3683.
141 E. Paleček, P. Boublíková and F. Jelen, Anal. Chim. Acta, 1986, 187, 99-107.
142 A. O. Brett and S. Serrano, J. Braz. Chem. Soc., 1995, 6, 97-100.
143 Y. Fan, K.-J. Huang, D.-J. Niu, C.-P. Yang and Q.-S. Jing, Electrochim. Acta, 2011, 56, 4685-4690.
144 S. Steenken and S. V. Jovanovic, J. Am. Chem. Soc., 1997, 119, 617-618.
145 C. E. Crespo-Hernández, D. M. Close, L. Gorb and J. Leszczynski, J. Phys. Chem. B, 2007, 111, 5386-5395.
146 E. Paleček, Electroanalysis, 1996, 8, 7-14.
147 P. M. Armistead and H. H. Thorp, Anal. Chem., 2000, 72, 3764-3770.
148 A. J. Bard, Electrogenerated chemiluminescence, CRC Press, 2004.
149 W. Miao, J.-P. Choi and A. J. Bard, J. Am. Chem. Soc., 2002, 124, 14478-14485.
150 E. E. Ferapontova and E. Domínguez, Electroanalysis, 2003, 15, 629-634.
151 E. Palecek and M. Bartosik, Chem. Rev., 2012, 112, 3427-3481.
152 X. Zhou, Q. Shen, K. Yuan, W. Yang, Q. Chen, Z. Geng, J. Zhang, X. Shao, W. Chen, G. Xu, X. Yang and K. Wu, J. Am. Chem. Soc., 2018, 140, 554-557.
153 B. Wu, H. Huang, J. Yang, N. Zheng and G. Fu, Angew. Chem., 2012, 124, 3496-3499.
154 L. Jin, B. Liu, S. S. Duay and J. He, Catalysts, 2017, 7, 44.
155 Z. Cao, D. Kim, D. Hong, Y. Yu, J. Xu, S. Lin, X. Wen, E. M. Nichols, K. Jeong, J. A. Reimer, P. D. Yang and C. J. Chang, J. Am. Chem. Soc., 2016, 138, 8120-8125.

